Validating and Understanding Feedbacks in the NCAR CSM

Climate feedbacks determine the sensitivity of the climate system to an external perturbation, affect the mean climate, and control the amplitude of natural variability. Thus validating and understanding feedbacks in climate models are of critical importance. Here we compare the feedbacks in CCM3--the amospheric component of the NCAR CSM--with those from observations over the equatorial Pacific cold-tongue. The results show that the net atmospheric feedback in the model over this region is strongly positive ($5.1 Wm^{-2}K^{-1}$) while in the real atmosphere it is strongly negative($-6.4 Wm^{-2}K^{-1}$). This discrepancy is largely due to errors in cloud feedbacks. Further noting a weaker surface heating over the cold-tongue in CCM3 than in observations, we suggest that the discrepancy in the atmospheric feedbacks may have contributed significantly to the cold biases in the equatorial Pacific in the NCAR CSM.

Results from Observations

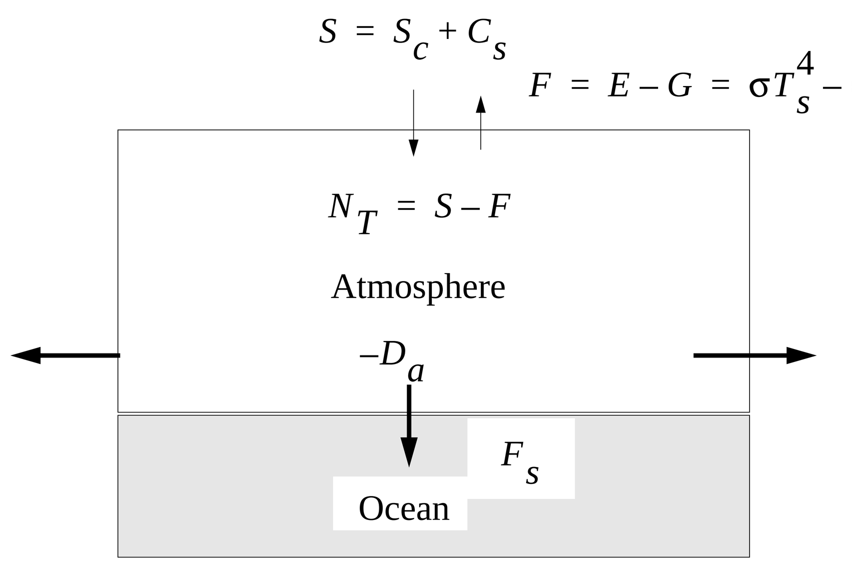

Figure 1: Physical processes in the atmosphere. S_c is the clear sky solar radiation, G_a is the greenhouse effect of water vapor, C_l is the greenhouse effect of clouds, C_s is the short-wave cloud forcing, N_T is the net radiative flux at the top of the atmosphere, D_a is convergence of moist static energy in the atmosphere, and Fs is the net surface heat flux into the ocean.

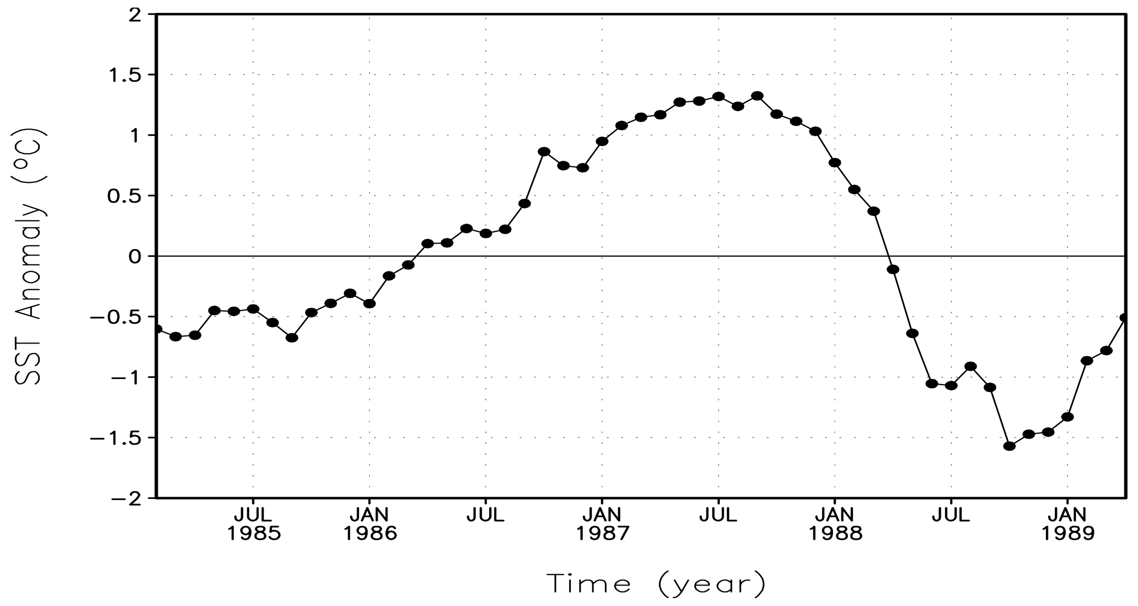

Figure 2: The SST signal. Shown is the time series of SST anomaly over the Pacific cold-tongue (5°S-5°N, 160°E-290°E).

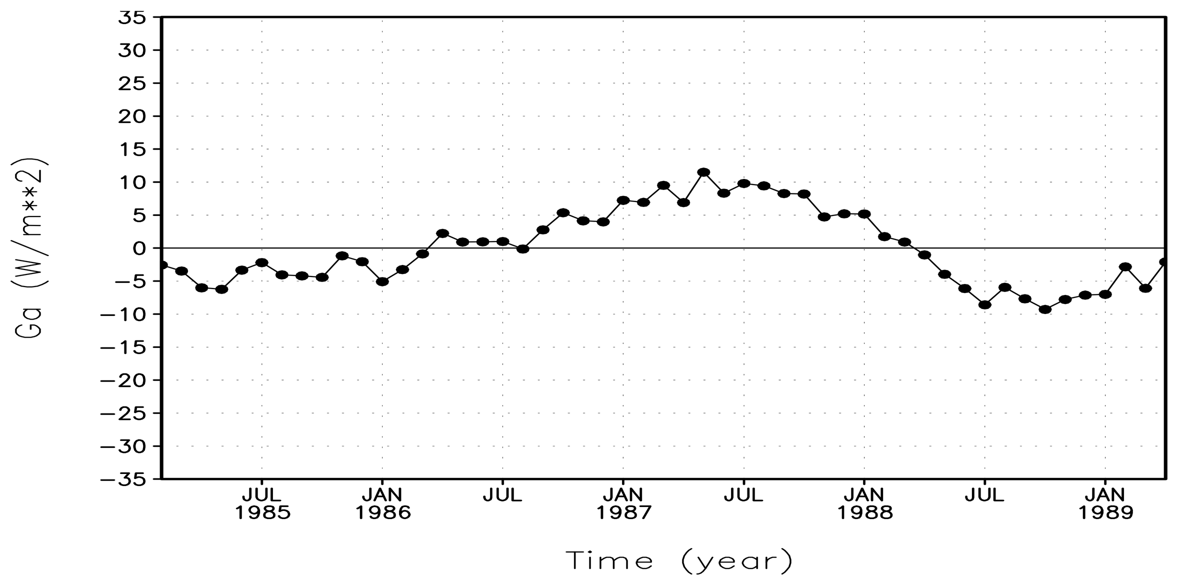

Figure 3: Response of the greenhouse effect of water vapor to the SST signal. Shown is the time series of G_a anomaly from ERBE over the Pacific cold-tongue.

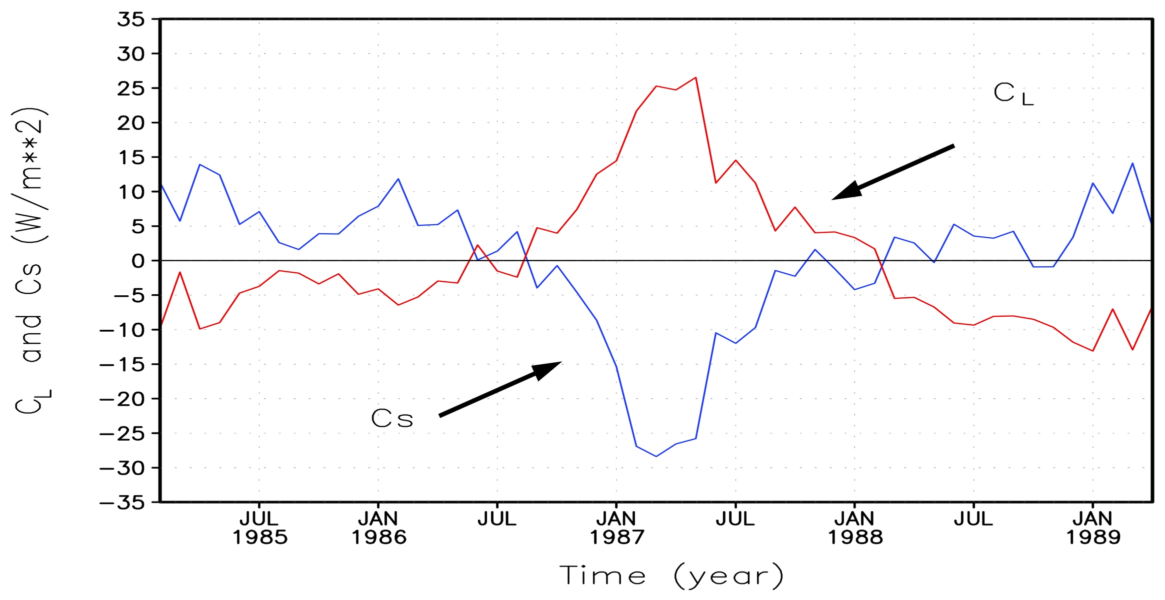

Figure 4: Response of the long-wave and short-wave forcing of clouds to the SST signal. Shown are time series of C_l and C_s from ERBE over the Pacific cold-tongue.

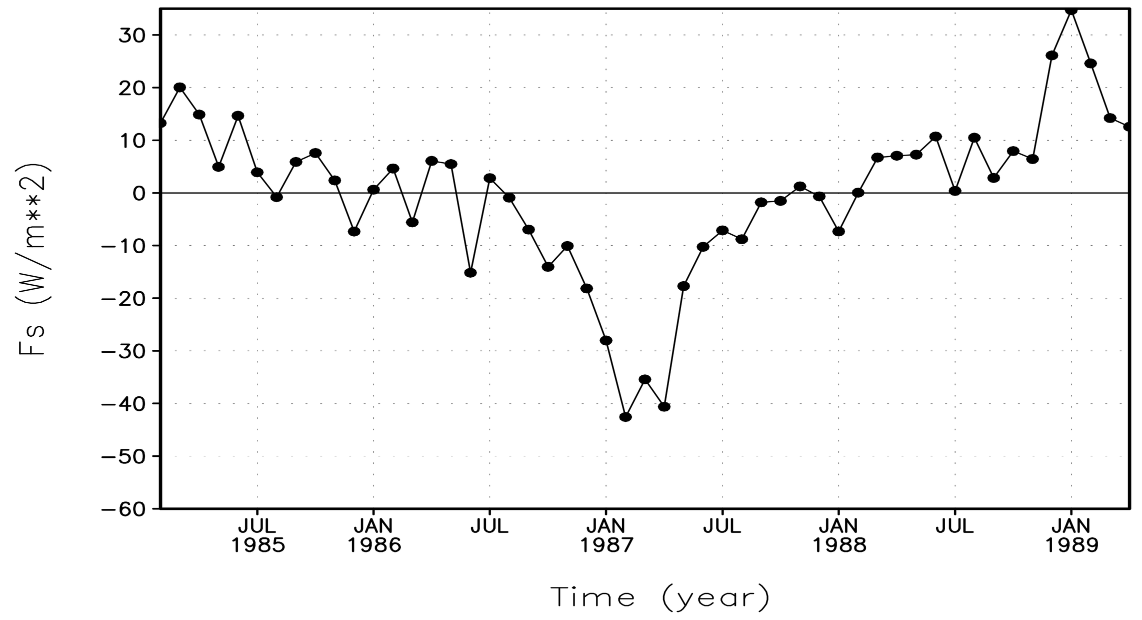

Figure 5: Response of the net equatorial heat flux into the ocean to the SST signal. Shown is the time series of F_s over the Pacific cold-tongue. Data for F_s are the same as in Sun and Trenberth (1998).

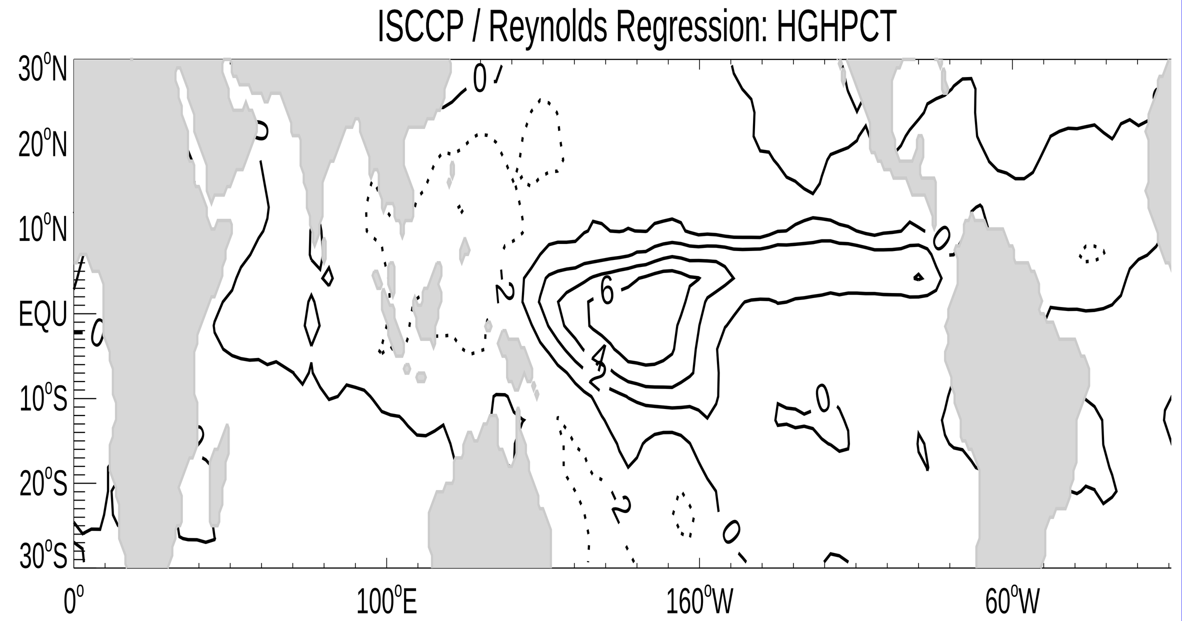

Figure 6: Response of the upper cloud cover to El-Nino warming in ISCCP data.

Results from NCAR CCM3

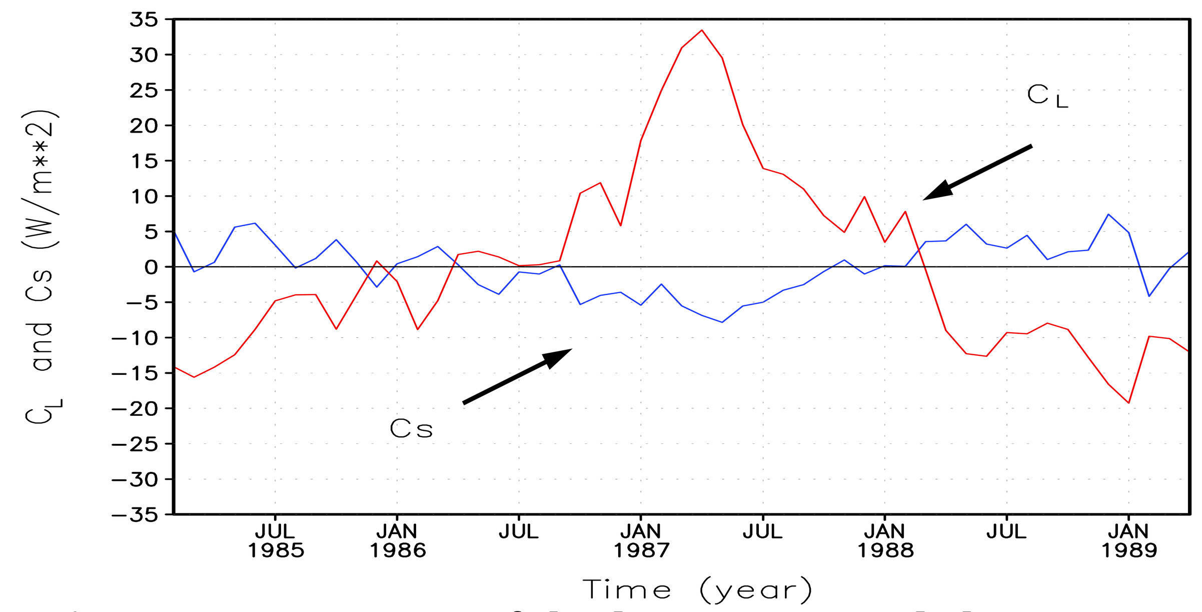

Figure 7: Response of the long-wave and short-wave forcing of clouds to the SST signal. Shown are time series of C_l and C_s from CCM3 over the Pacific cold-tongue.

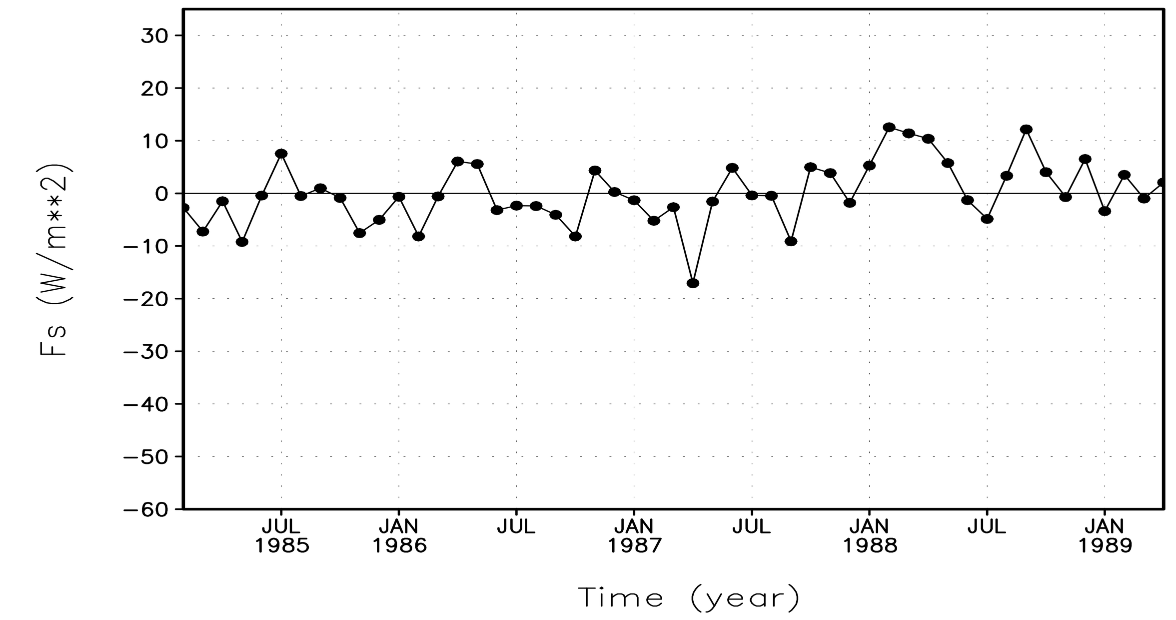

Figure 8: Response of the net equatorial heat flux into the ocean to the SST signal. Shown is the time series of F_s over the Pacific cold-tongue.

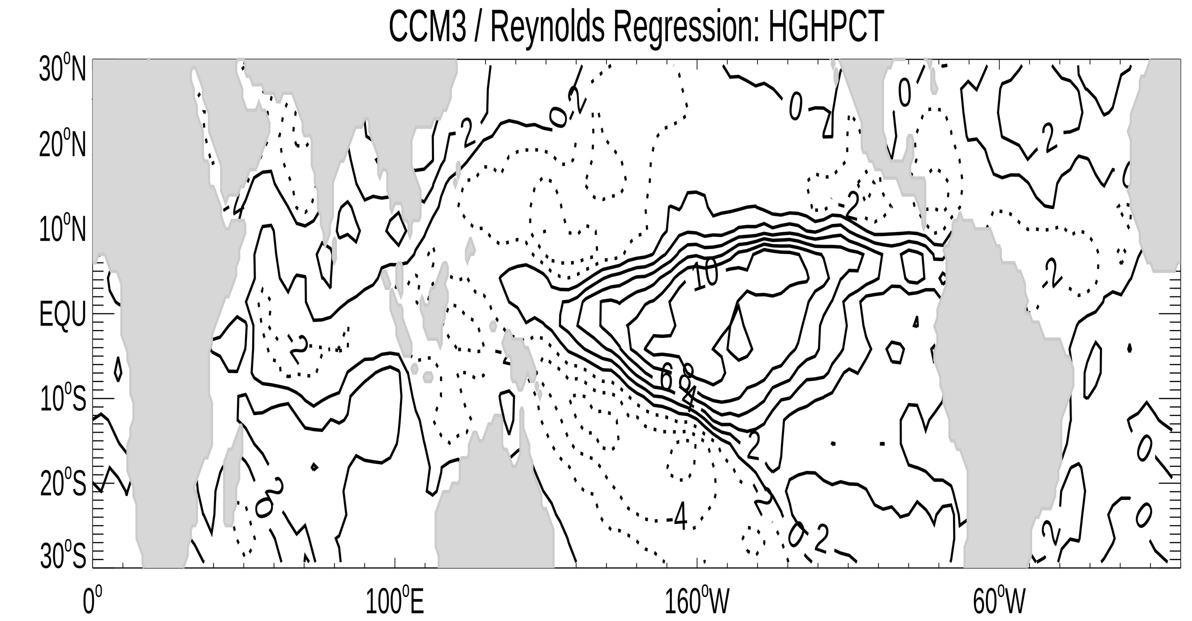

Figure 9: Response of the upper cloud cover to El-Nino warming in CCM3.

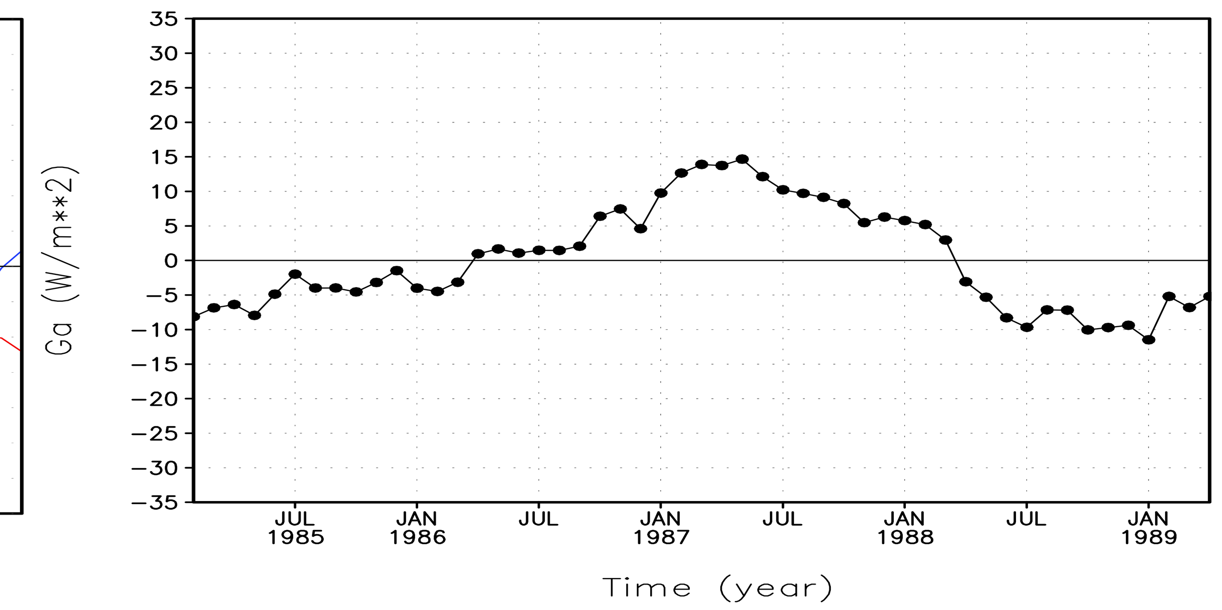

Figure 10: Response of the greenhouse effect of water vapor to the SST signal. Shown is the G_a interannual anomaly over the Pacific cold-tongue.

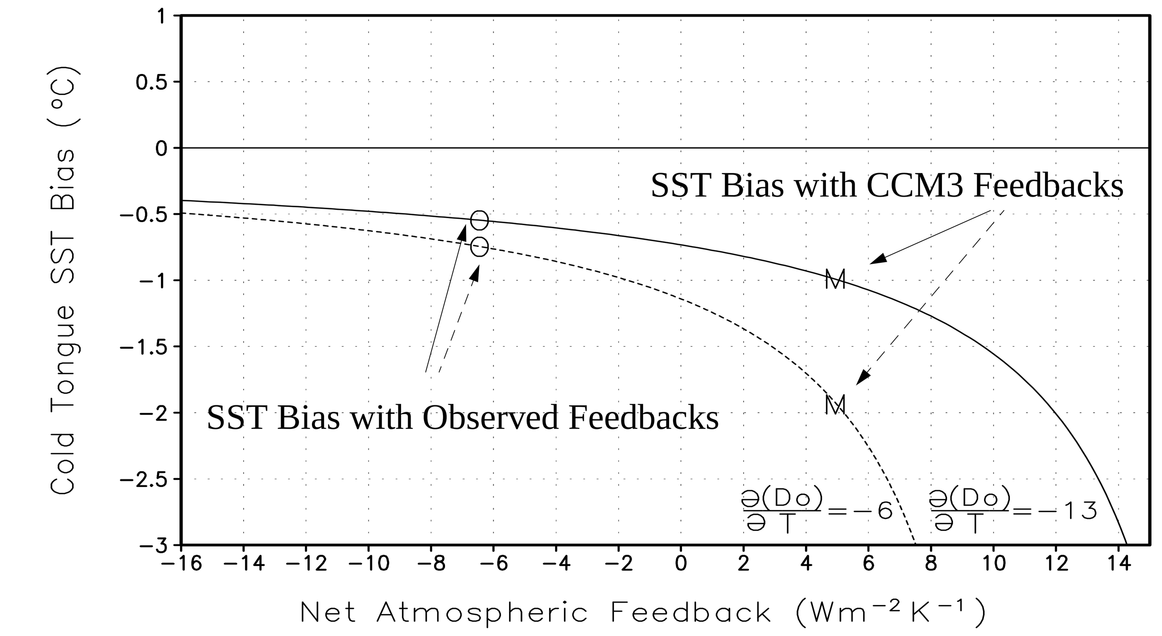

Figure 11: Cold-biases in equilibrium SST as a function of the net atmospheric feedback over the cold-tongue region. With the observed SST, the system is subject to a cooling of $14 Wm^{-2}$.

Atmospheric Feedbacks in NCAR CSM and Observations

Name of the Process	Feedback ($Wm^{-2}K^{-1}$)	
	Observations	Model
$\frac{\partial(G_a)}{\partial T}$	6.37 ± 0.23	8.26 ± 0.33
$\frac{\partial(C_L)}{\partial T}$	9.81 ± 0.88	12.96 ± 1.02
$\frac{\partial(C_S)}{\partial T}$	-7.79 ± 1.23	-2.98 ± 0.43
$\frac{\partial(D_a)}{\partial T}$	-14.80 ± 1.47	-13.18 ± 1.48
$\frac{\partial(F_A)^*}{\partial T}$	-6.41 ± 1.69	5.06 ± 0.96
$\frac{\partial(F_S)}{\partial T}$	-12.73 ± 1.72	-0.91 ± 0.96
$\frac{\partial(N_T)}{\partial T}$	2.37 ± 0.56	12.27 ± 1.12

* $\frac{\partial(F_A)}{\partial T} = \frac{\partial(G_a)}{\partial T} + \frac{\partial(C_L)}{\partial T} + \frac{\partial(C_S)}{\partial T} + \frac{\partial(D_a)}{\partial T}$

Table 1. Radiative and dynamic feedbacks from CCM3 and observations. The feedbacks are obtained through a linear regression.

De-Zheng Sun, John Fasullo, Tao Zhang, and Andres Roubicek, NOAA-CIRES/Climate Diagnostics Center, Boulder, CO
http://www.cdc.noaa.gov/~ds